

The Wideband Implantable Antenna with Circular Polarization for Monitoring the Thyroid

Jaya Prakash M., Kishore A., Shiyam P., Ramasamy K. and Sapna B. A.

*Department of Electronics and Communication Engineering, KIT-Kalaignarkarunanidhi Institute of Technology,
Coimbatore, Tamil Nadu, India*

Keywords: Implantable Antenna, Broadband, Circular Polarized Antenna, Thyroid Monitoring.

Abstract: A small circularly-polarized implantable antenna for long-term thyroid monitoring. The dual port loop structure proposed antenna covers a bandwidth of Wide band frequency 0.03 MHz - 6.02 GHz and it resonates at frequency of 2.45 GHz and 5.8 GHz which are mostly adopted for the WBAN and the medical telemetry applications. Antenna covers a super ultra-wide bandwidth due to the large operation band. An RO6010/droid 6010LM is selected as the substrate and the superstrate material within the compact design and its high dielectric constant and low loss are employed to minimize the size and improve the performance. The antenna footprint is 5 mm × 5 mm and its thickness are 0.57 mm in total. It demonstrates return losses of -22.45 dB at 2.45 GHz and -14 dB at 5.8 GHz. The antenna is -13dB (-19dB) at lower (upper) resonance frequency. SAR is studied by placing the antenna on the neck of human head model for human safety. The signal is well fastened yet dynamic in a dynamic environment, as a result of circular polarization. The simulation results exhibit satisfactory impedance matching and reasonable radiation efficiency, implying the proposed antenna is suitable to be used for the thyroid detection in biomedical applications.

1 INTRODUCTION

Implant antennas play a key role in biomedical applications, offering real-time health monitoring capabilities with minimal invasiveness. Recent research has demonstrated significant advancements in the design and performance of such antennas for deep-tissue applications. For instance, a study by Varvari (2024) focuses on the development of RF sensors for thyroid tracking, showcasing their effectiveness in early disease detection. Similarly, Asif introduced a wide-band tissue-deeply implantable antenna optimized for RF-powered medical devices, ensuring efficient signal transmission and power delivery. Metamaterial-based antennas have also gained traction due to their enhanced performance in miniaturized biomedical systems. Shaw (2019) explored a metamaterial implantable antenna with superior impedance matching and improved radiation efficiency. In the field of capsule endoscopy and deep-tissue monitoring, Shah (2024) developed four-port triple-band MIMO antenna, addressing the challenges of high-data-rate communication within human tissues. Additionally, Song proposed a dual-band circularly

polarized implantable antenna, ensuring robust signal transmission in biomedical telemetry applications. A comprehensive review by Jasim et al. (2025) highlights the various design considerations, fabrication techniques, and challenges associated with implantable antennas for biomedical applications. Their study provides valuable insights into the evolution of implantable antennas, emphasizing health considerations and geometric optimizations for enhanced biocompatibility and performance. An ultra-wideband compact meander line antenna for brain implants and biotelemetry application in 2.45 GHz ISM band is presented in 2024 by Mohan and Kumar. Their study demonstrates the feasibility of miniaturized, high-performance antennas for deep-tissue communication, reinforcing the need for advanced implantable antenna designs in biomedical applications. These advancements underline the growing importance of implantable antennas in medical diagnostics and treatment. This paper introduces a wideband implantable antenna tailored for thyroid monitoring, integrating circular polarization for improved signal stability. The subsequent sections detail the antenna's structural

design, performance analysis, and SAR evaluation to validate its suitability for biomedical applications. This paper introduces an implantable antenna with broadband capabilities for thyroid monitoring. The introduction section provides an overview of antenna types used in implantable devices. Segment 2 describes the structure of the proposed antenna. Segment 3 presents a detailed analysis of the antenna's performance, followed by the conclusion in Segment 4.

2 ANTENNA DESIGN

2.1 Antenna Structure

This implantable antenna is designed with a dual-port feeding mechanism is utilized within a symmetrical square layout of $5 \text{ mm} \times 5 \text{ mm}$ and a total thickness of 0.57 mm , shown in figure 1 making it well-suited for integration into space-constrained medical devices. Rogers RO6010/duroid 6010LM, selected for its high permittivity (10.2) and low dielectric loss, serves as both the substrate and superstrate, ensuring effective miniaturization and improved operational efficiency. The optimized dimensions are outlined in the Table 1.

Table 1: Parameters of Antenna.

Antenna Parameters	L	W	W1	W2	W3	L1	H
Dimension (mm)	5.0	5.0	0.30	1.0	0.20	0.850	0.254

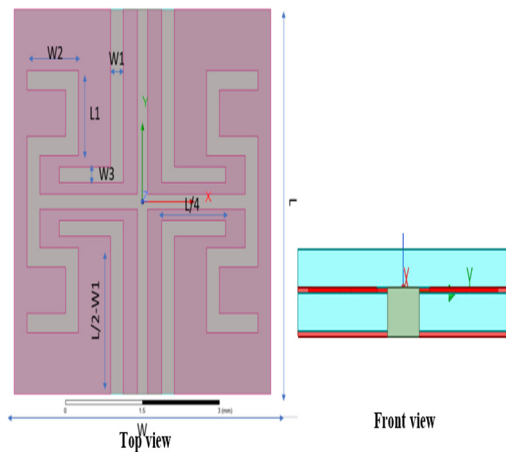


Figure 1: Patch and Port View.

2.2 Feeding Mechanism

A dual-port feeding mechanism is utilized, where rectangular strips interconnect at opposite ends to form a closed-loop structure. This configuration allows for precise excitation control, facilitating circular polarization with a broad bandwidth. The resulting stable wireless communication is critical for dynamic implantable applications.

2.3 Design Evolution

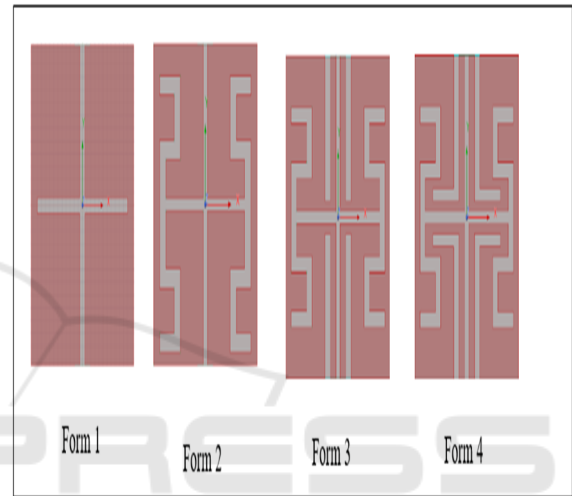


Figure 2: Top View of Antenna Across Each Iterative Cases.

The antenna design underwent four iterative modifications to refine its performance. The initial design used a Jerusalem cross-shaped patch, which was later optimized by introducing L-shaped and meandered slots to enhance impedance matching and return loss. The last incarnation had much better bandwidth and reflection coefficients. Each stage had a small change to the patch to improve the bandwidth, as well as the return loss of the antenna. The S_{11} for all four bands were compared as shown in Figure 3, evidencing a gradual performance improvement through the design procedure. The first patch had bad TLRL (return loss) due to high reflect and loss and only was excited at 5.58 GHz . Strategic cuts and variations of the dimensions of the patch in forms 2 and 3, resulted in an appreciative enhancement of return loss. The topology-double negative materials (DNGM)-TL SRR-R antenna and its parameters inherited from iteration 4 (form 4), as is embodied in figure 4, were designed, conducting a perfect impedance matching, over a wider range of higher frequencies from 39 kHz to 6 GHz with return loss of

-39.0 dB at 2.8 GHz and -43.0 dB at 5.36 GHz. Figure 2 shows Top View of Antenna Across Each Iterative Cases. The combined graph highlights the iterative enhancement purpose and confirms the success of design.

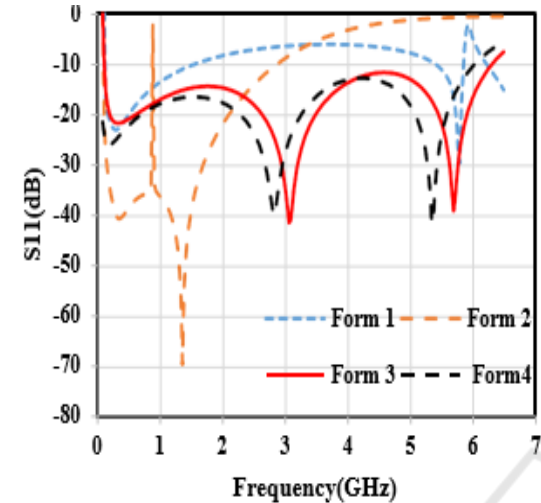


Figure 3: Iterative Levels Return Loss.

3 PERFORMANCE EVALUATION

3.1 Reflection Coefficient Analysis

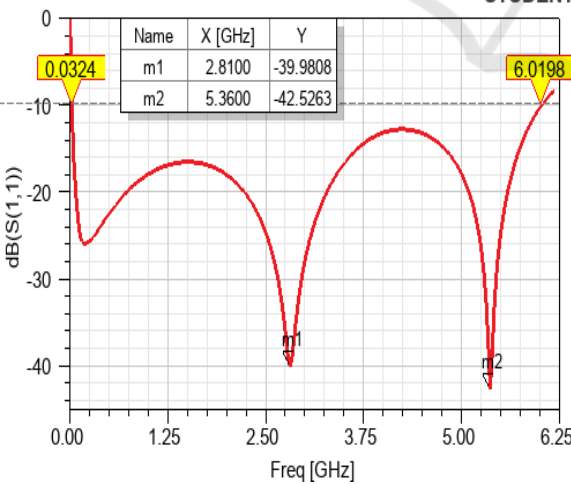


Figure 4: S11 Parameter.

Simulations conducted using HFSS confirmed the antenna performance in both free space and a phantom model simulating human tissue. The return loss values of -23.0 dB at 2.45 GHz also -14.0 dB at 5.8 GHz confirm a wide bandwidth extending from

0.03 MHz to 6.2 GHz. Figure 4 shows S11 parameter. The current flow plots illustrate the 180-degree phase shift, ensuring effective circular polarization displayed in Figure 5. The current direction changes by 180 degrees, indicating that the antenna operates with CP, which offers the advantage of easily sensing signals from all directions.

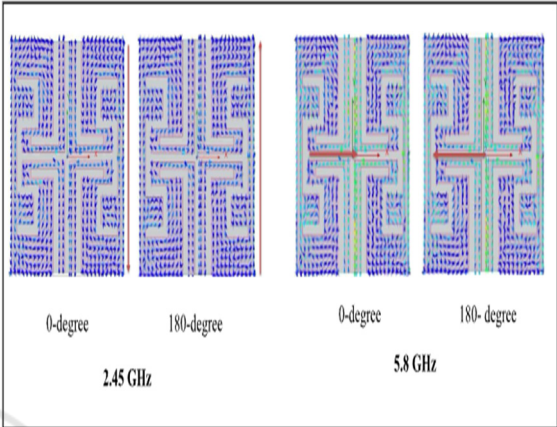


Figure 5: Flow of Current in the Antenna.

3.2 Radiation Performance

Figure 6 illustrates Radiation pattern simulations at the frequencies (as we mention in abstract) indicate stable circular polarization with minimal back. The gain performance of the antenna has been evaluated across its working frequency range, showcasing stable radiation characteristics. It achieves -19 dB and -13 dB ensuring reliable functionality within the intended frequency bands. Figure 7 shows Antenna Gain plot.

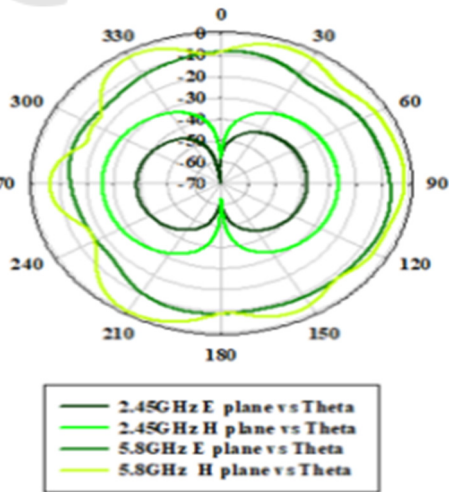


Figure 6: Field Pattern of the Antenna.

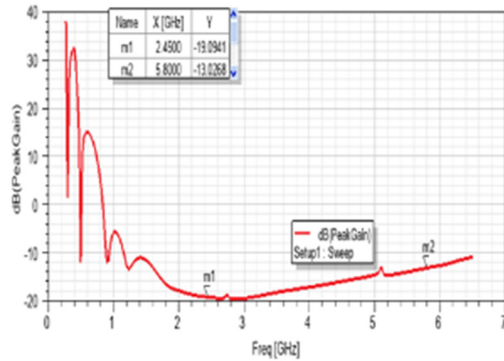


Figure 7: Antenna Gain Plot.

3.3 SAR (Specific Absorption Rate)

To ensure compliance with safety regulations, the specific absorption rate (SAR) was evaluated at input power levels of 1 W and reduced to maintain safe exposure limits.

The maximum SAR values of 1.59 W/kg at 2.45 GHz and 1.58 W/kg at 5.8 GHz confirm the design's suitability for biomedical applications with minimal

thermal effects on thyroid tissues. The input power was reduced, resulting in maximum allowable input power values of 5 mW at 2.45 GHz and 3.2 mW at 5.8 GHz. The simulated SAR, shown in Figure 8, was calculated using a human head phantom with the antenna placed in the neck region. The SAR analysis demonstrates that the antenna meets medical safety standards, effectively minimizing thermal impact on nearby thyroid tissues. Literature compared in Table 2.

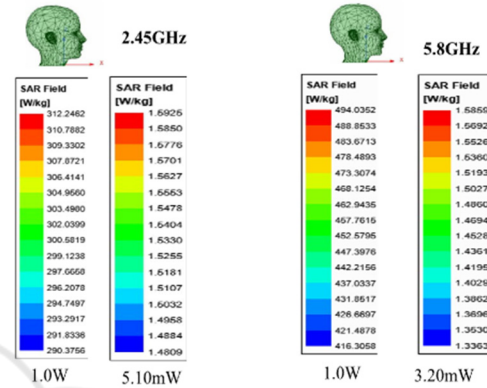


Figure 8: SAR Analysis of Antenna.

Table 2: Reference is compared with the antenna.

Ref. no	Freq (GHz)	Bandwidth	Dimension (mm ³)	Gain (dB)	SAR (W/kg)
1	5	300 MHz	13.38 × 18.24 × 1.52	5.8	NA
3	2.45	NA	12 × 12 × 3	-14.07	8.72
4	0.915	9.7%	10.5 × 7.5 × 0.127	-37.3	251
	1.780	7.8%		-30.3	211
	2.45	8.3%		-27.9	252
5	0.915	220 MHz	$\pi \times 0.0142 \times 0.0027$	-29.5	585.1
	2.45	230 MHz		-19.5	462.2
WORKED ANTENNA	2.45	5.97 GHz	5 × 5 × 0.57	-19.0	1.59
	5.8			-13.0	1.58

4 CONCLUSIONS

Wideband implantable antenna with circular polarization for monitoring the thyroid is operates across 0.03 MHz to 6.0 GHz offering a total bandwidth of 5.970 With compact dimensions of 5 mm × 5 mm × 0.57 mm, it ensures efficient integration within biomedical applications. The evaluation of both simulation and experimental results confirms optimal impedance matching, with S11 of -23.0 dB at 2.45 GHz and -14.0 dB at 5.8 GHz. SAR analysis validates with medical safety standards, maintaining maximum allowable power levels of 5.10 mW and 3.2 mW at the respective frequencies,

ensuring biocompatibility and minimal tissue heating. This study confirms the antenna's suitability for thyroid detection in biomedical applications, ensuring stable and secure wireless communication. Future advancements may focus on integrating it with implantable sensors and further reducing its size to expand its usability in diverse medical fields.

ACKNOWLEDGEMENTS

File No.8-122/FDC/RPS/POLICY-1/2021-2022.

REFERENCES

- Jasim, Mosab, et al. "An extensive review on implantable antennas for biomedical applications: Health considerations, geometries, fabrication techniques, and challenges." *Alexandria Engineering Journal* 112 (2025): 110-139.
- Mohan, Archana, and Niraj Kumar. "Implantable antennas for biomedical applications: a systematic review." *BioMedical Engineering OnLine* 23(1) (2024): 87.
- Mohan, Archana, and Niraj Kumar. "An ultra-wideband compact meander line antenna for brain implants and biotelemetry applications in the 2.45 GHz ISM band." *Results in Engineering* 24 (2024): 103345.
- Samanta, Gopinath, and Debasis Mitra. "Dual-band circular polarized flexible implantable antenna using reactive impedance substrate." *IEEE Transactions on Antennas and Propagation* 67(6) (2019): 4218-4223.
- Shah, Syed Manaf Ali, et al. "Four-port triple-band implantable MIMO antenna for reliable data telemetry in wireless capsule endoscopy and deep tissue applications." *IEEE Transactions on Antennas and Propagation* (2024).
- Varvari, Anna A., et al. "Thyroid Screening Techniques via Bioelectromagnetic Sensing: Imaging Models and Analytical and Computational Methods." *Sensors* 24 (18) (2024): 6104.
- Zada, Muhammad, Izaz Ali Shah, and Hyoungsuk Yoo. "Metamaterial-loaded compact high-gain dual-band circularly polarized implantable antenna system for multiple biomedical applications." *IEEE Transactions on Antennas and Propagation* 68(2) (2019): 1140-1144.